





## Article

# Bootstrapping Artificial Evolution to Design Robots for Autonomous Fabrication

Edgar Buchanan <sup>1,\*</sup> , Léni K. Le Goff <sup>2</sup> , Wei Li <sup>1</sup>, Emma Hart <sup>2</sup>, Agoston E. Eiben <sup>3</sup> , Matteo De Carlo <sup>3</sup> , Alan F. Winfield <sup>4</sup> , Matthew F. Hale <sup>4</sup>, Robert Woolley <sup>1</sup>, Mike Angus <sup>1</sup>, Jon Timmis <sup>5</sup> and Andy M. Tyrrell <sup>1</sup> 

<sup>1</sup> Department of Electronic Engineering, University of York, York YO10 5DD, UK; wei.li@york.ac.uk (W.L.); rw1445@york.ac.uk (R.W.); mike.angus@york.ac.uk (M.A.); andy.tyrrell@york.ac.uk (A.M.T.)

<sup>2</sup> School of Computing, Edinburgh Napier University, Edinburgh EH10 5DT, UK; L.LeGoff2@napier.ac.uk (L.K.L.G.); E.Hart@napier.ac.uk (E.H.)

<sup>3</sup> Department of Computer Science, Vrije Universiteit Amsterdam, 1081 HV Amsterdam, The Netherlands; gusz.eiben@gmail.com (A.E.E.); matteo.dek@gmail.com (M.D.C.)

<sup>4</sup> Bristol Robotics Laboratory, University of the West of England, Bristol BS34 8QZ, UK; alan.winfield@brl.ac.uk (A.F.W.); matt.hale@brl.ac.uk (M.F.H.)

<sup>5</sup> School of Computer Science, University of Sunderland, Sunderland SR1 3SD, UK; Jon.Timmis@sunderland.ac.uk

\* Correspondence: edgar.buchanan@york.ac.uk

Received: 30 October 2020; Accepted: 2 December 2020; Published: 7 December 2020



**Abstract:** A long-term vision of evolutionary robotics is a technology enabling the evolution of entire autonomous robotic ecosystems that live and work for long periods in challenging and dynamic environments without the need for direct human oversight. Evolutionary robotics has been widely used due to its capability of creating unique robot designs in simulation. Recent work has shown that it is possible to autonomously construct evolved designs in the physical domain; however, this brings new challenges: the autonomous manufacture and assembly process introduces new constraints that are not apparent in simulation. To tackle this, we introduce a new method for producing a repertoire of diverse but manufacturable robots. This repertoire is used to seed an evolutionary loop that subsequently evolves robot designs and controllers capable of solving a maze-navigation task. We show that compared to random initialisation, seeding with a diverse and manufacturable population speeds up convergence and on some tasks, increases performance, while maintaining manufacturability.

**Dataset:** The source code used for this study is available here: <https://bitbucket.org/autonomousroboticevolution/mdpi2020/>

**Keywords:** evolutionary robotics; autonomous robot evolution; autonomous robot fabrication; robot manufacturability

## 1. Introduction

This study is part of the Autonomous Robot Evolution (<https://www.york.ac.uk/robot-lab/are/>) project that is concerned with robots that can reproduce and evolve in the real world [1,2]. The long-term objective is to enable the evolution of an entire autonomous robotic ecosystem, where robots live and work for long periods in challenging and dynamic environments without the need for direct human oversight. The envisioned system has two features which, when combined, make it special and very challenging: it concerns the evolution of physical robots—not only simulated

ones—and it is not limited to the evolution of robot controllers (brains), but also concerns the evolution of the robots' morphologies (body plans).

The construction of a real-world robot is much more time- and resource-consuming than the construction of a digital robot, a piece of code that represents a robot in simulation. The difference can be huge; for instance making a robot in a simulator may take less than a second consuming only small amounts of energy, CPU power and memory, while building a real robot can easily take many hours and consume significant energy, raw materials and components. This means that each evolutionary trial should be considered carefully and should not be wasted. Secondly, further to the physical phenotype challenge, we have the fabrication challenge. That is, new robots do not just miraculously materialise, but need to be fabricated, and the fabrication process implies its own implementation-specific constraints. In an autonomous robot evolution system, automated fabrication is necessary, without human assistance. For example, the ARE project uses a 3D-printer, an 'organ bank' of prefabricated (non-printable) components and a robot arm that assembles all body parts to form a new robot (the phenotype) according to the given specification (the genotype). The operation of such an autonomous fabrication system is constrained by several practical details, e.g., the limitations of the 3D-printer, the shapes, sizes and interfaces of the prefabricated 'organs', and the position, size and geometry of the assembly arm. Thus, the essence of the fabrication challenge is that a robot needs to be not only conceivable but also manufacturable.

A potential solution for both challenges discussed above is the screening of robotic genotypes. To consider what this means, note that reproduction consists of two principal steps. Given two parent robots, the first step is to apply the crossover operator to their genotypes and produce a new genotype that encodes the offspring. This is a fully digital operation, hence relatively cheap. The expensive step is the second one, when the genotype-phenotype mapping is executed, in other words, when the physical robot 'child' is constructed. The idea of screening is to make the second step conditional by inspecting the new genotype, estimating the manufacturability of the corresponding robot and cancelling the fabrication of the phenotype if the outcome is negative. Obviously, manufacturability is not the only feature screening can consider. Specifically, it may be possible to rate the expected viability of a new robot, for instance, to check if it could move, or to estimate the (range of) its fitness value. Thus, in general, screening can take morphological properties, like manufacturability, as well as behavioural properties, like viability, into account.

Technically speaking, screening amounts to introducing constraints and a notion of feasibility regarding the search space. In the classic evolutionary algorithms (EA) literature, constrained optimisation problems can be handled in two different ways, (1) allowing infeasible solutions during the search, but using a penalty function, or (2) not allowing infeasible solutions and evolving in a feasible space. The first option is not applicable in this case because a solution that is not feasible means a robot that is not manufacturable.

The second option requires that evolution takes place in the feasible part of the search space. An essential prerequisite to this end is that the initial population consists of manufacturable robots. Furthermore, the initial population should be diverse, as this increases the probability of finding the best robots for the given environment and task. The main objective of this paper is to develop a method to generate both feasible and diverse initial populations.

The feasibility of physically fabricating evolved robots has been demonstrated by a handful of studies [3–7]. However, the robots in these studies are very simple; they have actuators to move, but they lack sensors to perceive the environment. In addition, constructing new robots is a very tedious process that relies much on human assistance. Only Brodbeck et al. [4] achieved the autonomous fabrication of robots at the cost of extremely simplifying the robot designs and the fabrication process: their robots consist of three to five cubes stacked upon each other and glued together, driven by an external computer. The ARE project works with complex autonomous robots with several different components, including a CPU, actuators, sensors and 3D printed complex shapes. The challenges of autonomous fabrication of robots in ARE have been highlighted in [2,8,9] where the

Robot Fabricator (the machine that fabricates robots) imposes different constraints in 3D printing and autonomous assembly.

This paper has two main contributions. First, a method to generate a diverse set of manufacturable and viable robots. Second, an assessment of the robots this method delivers from two perspectives, (a) their learning potential and (b) their evolutionary potential. For (a), a controller is learned for each body plan in the bootstrap population. For (b), we use them as the initial population for an artificial evolutionary process. For this investigation, we consider three environments concerning navigation.

The approach and experimental workflow is summarised in Section 3. Firstly, a novelty search algorithm is used to produce a large and diverse pool of body plans. Three body plan descriptors (vector describing specific features of the robots) are compared to find the most efficient way to explore the search space. Then, a population of robots is selected from this pool. Four selection processes are compared based on their capacity to produce the most diverse population. This population is evaluated in a maze navigation task with randomly-sampled controllers and learned controllers for each body plan in the population. Finally, the population of body plans is used to bootstrap an evolutionary process. To assess the benefit of using this bootstrap population, the same experiments are also conducted with a randomly sampled population.

The specific research questions investigated are the following:

1. What is the best combination of descriptor and selection method to maximise the diversity of body plans in the bootstrap population?
2. What are the benefits of evolving a diverse bootstrap population over simply randomly sampling from the space of body plans?
3. Are the robots formed by the bootstrap population more capable of solving a navigation task than a randomly sampled population (when combined with method(s) to learn a controller)?

The key results from this paper are that the use of bootstrap population is beneficial for (a) the generation of a population of robots diverse enough to produce robots capable of solving simple environments; and (b) reduce the number of evaluations required to converge to the solution when evolution is used. Most importantly, this method aids to overcome the challenges of finding body plans in a difficult landscape constrained by the limitations of autonomous robot fabrication.

This paper extends the results from [9] by investigating additional alternative descriptors to determine which descriptor is most efficient. This paper has the following novel additional contributions.

1. An investigation was carried out on various selection methods to determine which robots were selected to form an initialised population.
2. The behavioural potential in each evolved robot of the population was evaluated by using a controller learning mechanism in three different environments.
3. The body plans and controllers were evolved simultaneously, starting with a bootstrapped population and a random population in three different environments.

## 2. Related Work

As outlined above, the idea of evolving the body plans for “virtual organisms” or “robotic lifeforms” has been around for decades, but existing work is limited to conducting evolution in computer simulations. The long-term vision regarding physically embodied artificial evolutionary systems has been first outlined in 2012 by Eiben et al. who described the main concepts and discussed the related promises and challenges, but provided no specific guidelines for actual implementations [10]. Such guidelines were given in [11] that presented a generic system architecture, named the Triangle of Life (ToL) for “robots that evolve in real-time and real-space”. The Triangle of Life framework is illustrated on the left-hand side of Figure 1. It consists of three principal stages: morphogenesis, infancy and mature life. Consequently, a tangible implementation consists of three

main system components: the Robot Fabricator, the Training Facility and the arena. The Robot Fabricator is where new robots are created. The Training Facility hosts a learning environment for ‘infant’ robots so they can learn to control their—possibly unique—body to acquire basic skills (e.g., locomotion, object manipulation) and to perform more complex tasks. If a robot achieves a satisfactory level of performance, it is declared a fertile adult and enters the arena (which represents the world where the robots must survive and perform user-defined tasks) and is considered a viable candidate for parenthood.

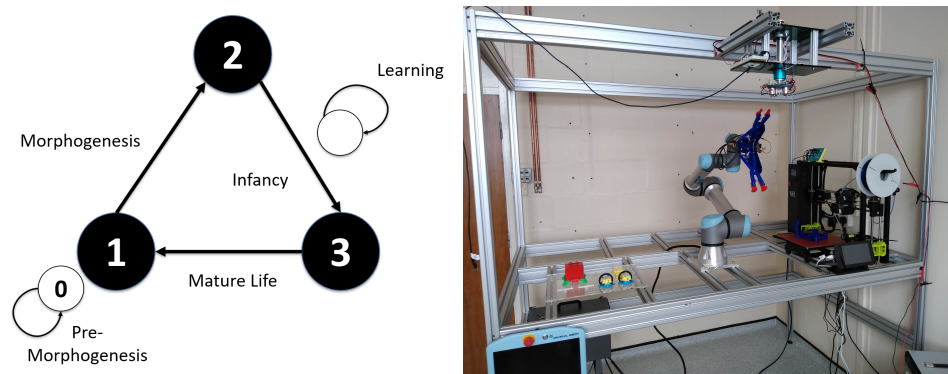


**Figure 1.** Triangle of life (left) and Robot Fabricator (right).

The autonomous robot fabrication in the Robot Fabricator has many challenges. It is easy to see why this is an important issue if we are to evolve physical robots: the resources are much more limited than in ‘simple’ computer simulations. Minimising resources is important because constructing a robot is expensive and even though the initial population is random, one should not waste resources, and should also make sure that the robots therein are individually transferable to reality and the population as a whole is transferable. The transferability of an individual robot can be defined through morphological or behavioural properties [12]. Regarding body plans, the phenotype is required to be manufacturable.

This study is directly linked to the reality gap issue widely studied in evolutionary robotics (ER). The manufacturability constraints define robots that are transferable to reality. Most of the work in the literature on crossing the reality gap in ER addresses the behaviour of the robots. Different approaches have been proposed in literature, from (1) optimising the simulator to get closer to reality [13,14] or (2) simplifying the simulator to target the most important aspects of the task, thus narrowing the gap [15] or (3) producing a large list of diverse behaviours and choosing the suitable behaviour according to the current situation [16]. The closest approach to the present study is the transferability approach described in [12]. This approach aims at finding measures to assess the similarities/differences between a controller running on a simulated robot and its physical counterpart. In this study, manufacturability is considered to be analogous to transferability, but applied to body plan designs. In terms of considering manufacturability of physical robots, one other approach is worthy of mention: recent work by Kriegman et al. [6] describes a pipeline for creating living robots made from cells using an evolutionary process. Designs created by simulated evolution are first passed through a robustness filter which filters out evolved designs with behaviours that are not robust to noise, and then through a build filter [6] which removes designs that are not suitable for the current build method or unlikely to scale to future tasks. Surviving designs are then hand built. A significant difference to the method proposed in this paper is that the filters are applied post-evolution and are not accounted for in any way during the evolutionary process.

In this paper, a new method for population initialisation of diverse and manufacturable robots is proposed. The objective of population initialisation in EAs is to provide an initial guess of solutions, and then this population will be iteratively improved over time. However, recent studies have shown that a good selection of the initial population can increase the probability of finding the global



optima and decrease the time it takes to find it [17]. Different strategies have been proposed in the literature with different results, and a survey of this literature can be found in [18]. Nonetheless, to our knowledge, no strategies of population initialisation of robots that can be autonomously constructed have been explored in ER.

### 3. Experimental Framework

The experimental framework followed for this paper is shown in Figure 2. Firstly, a large pool of diverse robots is evolved. Then, from this pool, a smaller subset of robots is selected as initial population, referred to as ‘bootstrap population’ in this paper. Finally, the capability of the body plans to solve a navigation task is measured with randomly-sampled controllers and learned controllers. In addition, the bootstrap population is tested with an experiment where the body plans and the controllers are further evolved to solve a navigation task.

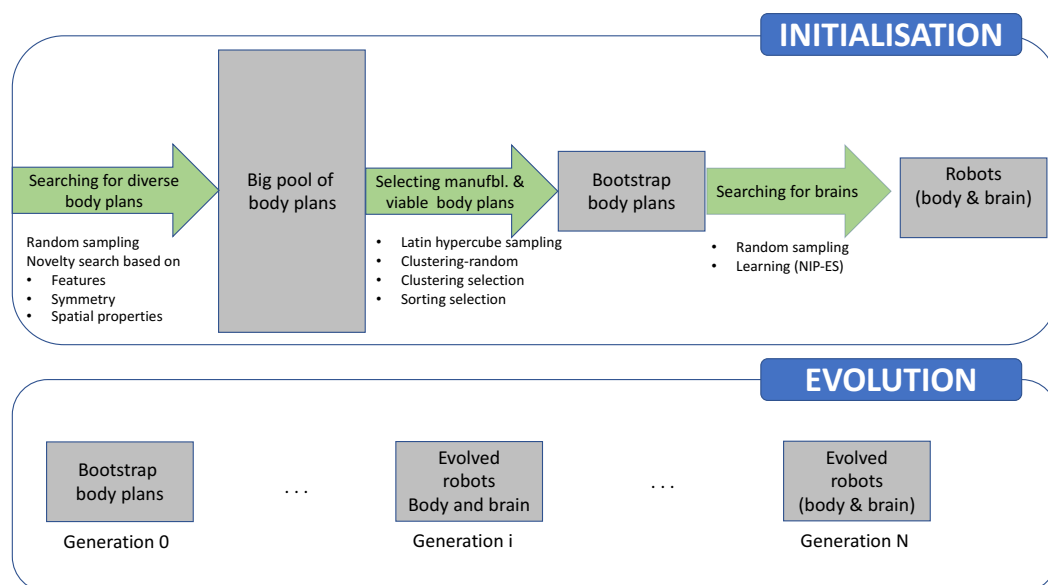


**Figure 2.** Overall system diagram. Upper image: Initialisation process. Firstly a large pool of robot body plans is generated, aiming for diversity. Then a subset of these body plans is selected focusing on manufacturability and viability. In the third step, controllers are generated for these body plans to form complete robots. Lower image: Evolutionary process. The robots from the bootstrap population are evolved.

#### 3.1. Generation of a Large List of Diverse Body Plans

The main objective of this stage is to generate a large list of diverse robots that are also manufacturable. Therefore, one of the goals of this section is to identify the body plan descriptor that maximises diversity when the robots are evolved.

##### 3.1.1. Body Plan Generation

The body plan generation used in this paper is a variation of the one introduced in [9]. The robots have two types of components: skeleton and organs. The skeleton is the 3D-printable structure that holds the robot together. Organs are the active or passive pre-fabricated components. The organs used in this paper are the head, joint, wheel, sensor and castor organs all shown in Figure 3 and described next.

- The head organ takes the role of receiving signals from the sensors and sending signals to the actuators (and includes the power source).

- The joint organ is an actuator which takes frequency as an input and outputs the position of the actuator in the interval from  $-90$  to  $90$  degrees.
- The wheel organ is a rotational actuator which takes velocity as an input.
- The sensor organ can output two different signals. The first signal is distance to the closest obstacle. The second signal is binary where the signal is 1 if the beacon is detected, or 0 if the beacon is not detected and it might be occluded by an obstacle.
- The castor organ is a passive component which reduces the friction of the robot with the floor.

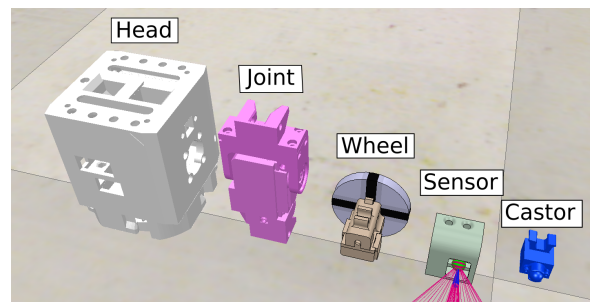


**Figure 3.** Each body plan has one head organ and could have one or more joint, wheel, sensor and castor organs.

The body plans are encoded in a Compositional Pattern Producing Network (CPPN) first introduced by Stanley [19], as it has been demonstrated that with this encoding it is possible to evolve complex patterns. The structure of the CPPN has 4 inputs and 6 outputs. The four inputs define the position of a cell in a 3D matrix with size  $13 \times 13 \times 13$  mm, where the first three inputs are the coordinates  $x$ ,  $y$  and  $z$ , and the last input is the distance  $r$  from the centre of the cell. The six outputs define the properties of each cell in the 3D matrix. The first five outputs are binary and they represent the absence or presence of a specific type of voxel. There are five types of voxels: skeleton, wheel, sensor, joint and castor. The last output represents the rotation of a specific component around the normal of the surface of the skeleton.

The genotype to phenotype decoder operates as follows:

1. Firstly a single layer skeleton 'seed' is generated around the head organ. After this, the skeleton output is queried for the entire 3D matrix. This will generate the plastic connecting all the organs. Only one region of skeleton is allowed per body plan, where a region is a cluster of inter-connecting skeleton voxels. The biggest region of skeleton is preserved and any regions unconnected to the 'seed' are removed.
2. Then, the CPPN is queried to determine wheel, sensor, joint and castor outputs, generating multiple regions for each type. An organ is generated in each intersecting area between the organ region and the skeleton surface. This ensures that all the components are connected to the surface of the skeleton. Only one component is generated in each region regardless of the size of the intersecting area.
3. Two relative rotations of the organs are given by the normal of the skeleton surface. The third rotation around the relative axis of the organ is given by the last output of the CPPN.

As mentioned in the introduction, the Robot Fabricator, shown in Figure 1, imposes various constraints on the body plans that can be manufactured. These constraints are listed below and shown in Figure 4:

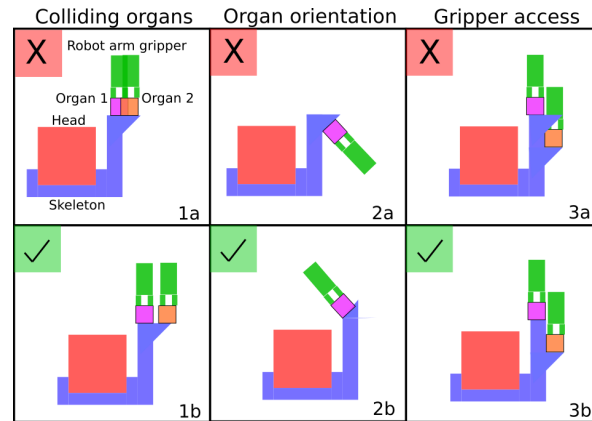


**Figure 4.** This figure shows the constraints imposed by the Robot Fabricator. The top row shows some examples of invalid body plans and the bottom row shows valid examples of body plans. If one of the organs violates at least one of these constraints, that organ is removed from the final body plan.

- Colliding organs—Body plans evolved in simulation should not have overlapping components (Figure 4-1).
- Good organ orientation—The organs are attached to the skeleton through male-female clip connectors where the male connector is always generated on the skeleton. The male connectors should not be pointing downwards as supporting material would then be required during printing. This supporting material would act as an obstruction during the process of robot fabrication.
- Gripper access test—The robot arm should have clear access to attach the organs. In other words, there should not be any obstacles in the way of the robot arm (Figure 4-3).

With these constraints in mind, if one or more organs violate at least one of these constraints, they are removed from the final body plan.

Some examples of body plans evolved can be found in the video in [20]. A video of the Robot Fabricator assembling a robot can be found in [21].

### 3.1.2. Body Plan Descriptors

The aim of the body plan generation experiments is to generate a large diverse list of robots. For this, the novelty search algorithm is used. The novelty search algorithm [22] replaces the traditional fitness function with one which rewards novelty. Novelty is measured by comparing a descriptor vector (which describes the body plan represented by an individual) with the descriptors of both the current population and those maintained in an archive produced by the same algorithm and described below (more details in Appendix A):. In this paper we extend the work in [9] where body plans were evolved for a single descriptor. For this paper three different descriptors are compared: the *feature* descriptor, *symmetry* descriptor and the *spatial* descriptor. These descriptors are described next.

#### Feature Descriptor

The objective of this descriptor is to capture the features of a body plan with a low number of traits. In this case the descriptor, shown in Equation (1), contains 8 traits:

- The *width*, *depth* and *height* traits describe the volume of the robot.
- The number of *voxels* represents the voxels used for the skeleton in the body plan.
- The number of *wheels*, *sensors*, *joints* and *castors* traits represent the final number of these components in the body plan

$$x = [\text{width}, \text{depth}, \text{height}, \text{voxels}, \text{wheels}, \text{sensors}, \text{joints}, \text{castors}] \quad (1)$$

### Symmetry Descriptor

For the *symmetry* descriptor, Equation (2), the body plan is divided in 8 quadrants which follows the coordinate system, where the centre of this coordinate system is in the middle of the 3D matrix. Then, each trait in the vector counts the number of *voxels*, *wheels*, *sensors*, *joints* and *castors* in each of the 8 quadrants.

$$x = [\text{voxels}_0, \text{voxels}_1, \dots, \text{voxels}_7, \text{wheels}_0, \text{wheels}_1, \dots, \text{wheels}_7, \text{sensors}_0, \text{sensors}_1, \dots, \text{sensors}_7, \text{joints}_0, \text{joints}_1, \dots, \text{joints}_7, \text{castors}_0, \text{castors}_1, \dots, \text{castors}_7] \quad (2)$$

### Spatial Descriptor

The *spatial* descriptor, Equation (3), is the largest, and it encodes the content of each cell in the 3D matrix of the final body plan after generation. Each cell could have one of 6 different values: empty cell, skeleton or an organ type (wheel, sensor, joint or castor).

$$x = [\text{Cell}_0, \text{Cell}_1, \dots, \text{Cell}_{2196}] \quad (3)$$

#### 3.1.3. Experiments and Results

The main goal of the experiments in this section is to compare the different body plan descriptors introduced in the previous section in order to identify the descriptor that provides the most diverse set of body plans. For this, qualitative and quantitative results are shown. A total of 30,000 robots were produced for random sampling and for each body plan descriptor. A total of 20 replicates or repetitions are shown in these results.

Figure 5 shows some examples of robots produced with *random sampling* and evolved with each descriptor. The robots produced with *random sampling* have simple skeletons (basic shapes) with a low number of organs. The random generation of CPPNs is not capable of creating patterns that create complex skeletons and robots with a high number of organs. Robots evolved with the *feature* descriptor have the highest number of organs, but the skeletons are simple. Since half of the attributes of this descriptor measure the number of organs, the body plans are evolved with more organs. Robots evolved with the *symmetry* descriptor have a higher number of organs with more complex skeletons. Robots evolved with the *spatial* descriptor have the most complex skeletons with the lowest number of organs. This is because the number of skeleton-related traits outweighs the traits for organs in this descriptor.

As for quantitative results, the total number of robots with given number of organs is shown in Table 1. The *feature* descriptor generates the highest number of robots with different numbers of organs. The *spatial* descriptor generates the list of robots with the lowest number of organs. This means that the *feature* descriptor will have a greater probability of producing robots with the necessary organs to solve the given task.

The mean sparseness for each descriptor is shown in Table 2 and measured using Equation (A1). Unsurprisingly, the highest sparseness value associated with each list of robots comes from the descriptor used to evolve the list. This corroborates the finding that each list of robots is diverse according to the descriptor that they were evolved with.

The exploration space coverage is shown in Table 3. The coverage is measured by discretising the exploration space into bins, in this case 5 bins per dimension. The coverage measures the ratio of bins covered. The coverage is only measured for the *feature* descriptor, as with the given number of body plans the coverage is very small for the other descriptors. In addition, it takes significantly more time to calculate the coverage for the other descriptors. As expected, the *feature* descriptor has the highest coverage but with the *symmetry* in close second. The coverage is very small due to the size of the exploration space and the low number of body plans.



**Figure 5.** Body plans generated with *random sampling* and evolved with each descriptor (feature, symmetry and spatial). The descriptors define the final features in the robots. The feature descriptor generates the robots with highest number of organs and low skeleton complexity. The spatial descriptor generates the robots with the lowest number of organs but with high skeleton complexity. The symmetry descriptor sits in the middle of the previous descriptors.



**Table 1.** Each cell in this table shows the median number of robots with the number of organs specified in each row for the specified organ type in each column. The best values are highlighted. The *feature* descriptor generates the highest number of robots for different numbers of organs.

Organs		Random Sampling				Evolved with Feature Descriptor			
Number		Wheels	Sensors	Joints	Castor	Wheels	Sensors	Joints	Castor
0		28,504.5	28,236	28,059	27,242	23,311.5	23,056	22,620.5	21,247
1		1516.5	1786	1963.5	2783	6237	6585.5	6971.5	7878
2		2.5	4	2.5	6.5	419	536	488.5	847.5
3		0	0	0	0	25	25	31	158
4		0	0	0	0	0	0	0	6.5
Evolved with symmetry descriptor					Evolved with spatial descriptor				
0		23,961.5	23,031	22,108	19,945.5	29,362	28,973.5	28,788.5	28,364.5
1		5893.5	6828	7537.5	9079	662.5	1051.5	1236	1667.5
2		137.5	205.5	324	860.5	0	0	0.5	1.5
3		0.5	6.5	4.5	118.5	0	0	0	0
4		0	0	0	14	0	0	0	0

**Table 2.** Sparseness comparison table. Highlighted cells represent best values. Each descriptor has the highest sparseness when measured with the the same descriptor.

		Mean Sparseness ( $\times 10^{-3}$ ) Measured with		
		Feature	Symmetry	Spatial
Descriptors evolved with	Random			
	sampling	5	60	140
	Feature	10	60	99
	Symmetry	8	86	114
	Spatial	2	34	206

**Table 3.** Coverage comparison table. Shaded cells represent the best values. The feature descriptor has the highest coverage.

		All Dimensions		Only Organs	
		Coverage ( $\times 10^{-3}$ )	Uniformity of the Distribution	Coverage ( $\times 10^{-2}$ )	Uniformity of the Distribution
Random	sampling	1.87	0.33	2.24	0.32
	Feature	2.89	0.34	5.44	0.30
Evolved	Symmetry	2.83	0.34	5.28	0.33
	Spatial	0.77	0.32	1.28	0.32

In conclusion, each descriptor produces a different set of robots with different numbers of organs and skeleton complexity. For the navigation task it is desirable to have the highest number of robots with different numbers of organs rather than skeleton complexity. This is because this will increase the likelihood of finding the robot that completes the task. With this in mind, the *feature* descriptor provides the highest number of robots with different numbers of organs. The *feature* descriptor is used for the rest of the experiments in this paper.

### 3.2. Bootstrap Population Selection

After a large number of robots has been evolved, a smaller group of robots, the bootstrap population, needs to be selected to initialize a second evolutionary loop. The robots in this group should be diverse as this will increase the probability of finding the robot that is best suited for the task.

In order to ensure all the robots have some capability of exhibiting a behaviour, all the robots with at least one sensor and one actuator (wheel or joint) are extracted from the complete list of robots. The selection method is applied to this subset of robots. For the selection of this population, four different methods are compared.

- *LHS*—For this method, Latin hypercube sampling (LHS) [23] is used to select at random 100 body plans from the list of robots.
- *Clustering-random*—K-means clustering algorithm [24] is used to classify all the body plans into 100 groups according to the features of the morphological descriptor. After this, a random robot is sampled from each group.
- *Clustering-selection*—Similar to the *clustering-random* method, but instead of taking a random robot from each group, the robot with the highest sparseness value of the group is taken.
- *Sparseness-selection*—In this method, all the robots are sorted from the least sparse to the most sparse robot. Here the top 100 most sparse robots are used as the population.

### 3.2.1. Experiments and Results

The objective of the experiments in this section is to identify the selection method that generates the most diverse population from the list of robots evolved with the *feature* descriptor described in the previous section. For this, four different selection methods, introduced in this section, are evaluated: *LHS*, *clustering-random*, *clustering-selection* and *sparseness-selection*.

The mean sparseness for each selection method is shown in Table 4. All the robots in the bootstrap population for all the methods have at least one sensor and one actuator (wheel or joint) and this is because of the filter applied to ensure robots have enough components to exhibit a behaviour. *Cluster with random sampling* has the population with the highest sparseness ( $p < 0.05$ ) compared with *LHS* and *sparseness-selection*. There is no significant difference between *clustering-random* and *clustering-selection*.

**Table 4.** Mean sparseness comparison between selection methods. The u-test reveals that the *clustering-random* and *clustering-selection* have the greatest performance, with no significant difference between the two. Shaded cells represent the best value.

<i>LHS</i>	<i>Clustering-Random</i>	<i>Clustering-Selection</i>	<i>Sparseness-Selection</i>
0.41	0.425	0.424	0.4

The number of robots with different numbers of organs is shown in Table 5. The *LHS* method generates the lowest number of robots with different numbers of components. The *clustering-random* generates the highest number of robots with different numbers of organs, with *clustering-selection* in close second.

**Table 5.** Number of robots with different numbers of organs. Latin hypercube sampling (*LHS*) has the least diverse robots. The clustering methods have the most diverse robots. Shaded cells represent the best values.

#	<i>LHS</i>				<i>Clustering-Random</i>				<i>Clustering-Selection</i>				<i>Sparseness-Selection</i>			
	W	S	J	C	W	S	J	C	W	S	J	C	W	S	J	C
0	44	0	38	63.5	41	0	39.5	59	40	0	39.5	59.5	39	0	36.5	59
1	53.5	95	56.5	32.5	53.5	91	58	35.5	53.5	91.5	58	34	55.5	95.5	56	34
2	2.5	5	2	1.5	3	7.5	3.5	3	2.5	7.5	2.5	3	5	4.5	3	3.5
3	0	0	0	1	0	1	0	1	0	1	0	1	0	0	0	0

As mentioned in the results from the previous section, for the robots to solve the navigation task, it is desirable to have a range of robots with different numbers of organs, and for them to be diverse. The *clustering-random* and the *clustering-selection* methods provide the most diverse populations. For this reason, the populations selected by *clustering-random* will be used for the next set of experiments.

### 3.3. Evaluating Body Plan Potential by Adding a Controller

The objective of this stage is to determine the *potential* of a body plan by trying to learn a controller for the robot in a number of maze-navigation scenarios. These experiments also enable insight to be gained into which features of body plans correlate with their ability to solve a task.

In this navigation task, the robot starts at the origin and has to reach a target. At the target there is a beacon. The robots are evaluated in three different environments (Figure 6): *empty arena*, *escape room* and *middle wall*. Each of these environments will illuminate the necessary key features in the robots to solve each of the environments. For instance, for the *empty arena*, any body plan with actuators has a good probability of solving the task, whereas, in the *escape room*, the robots will need to have sensors to avoid the walls and be small enough to move through the gaps in the walls. In each experiment, the robot is controlled by an Elman neural network [25].

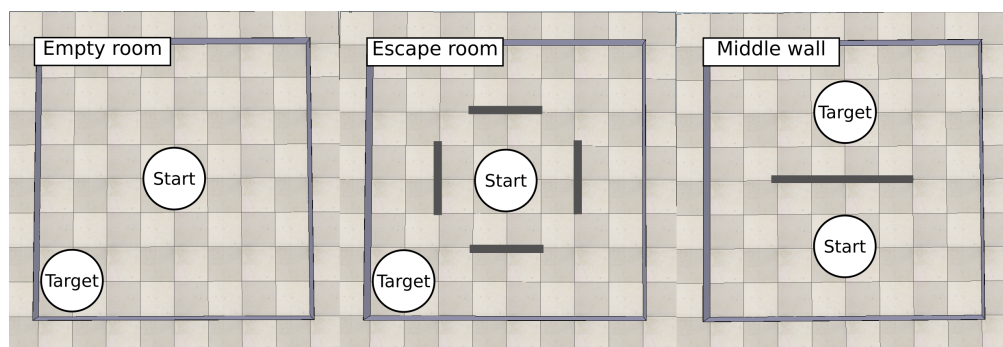


**Figure 6.** Environments used for the experiments in this paper: *empty arena*, *escape room* and *middle wall*. Each robot has to reach the target from the starting point. The size of the arena is  $2 \times 2$  m. In each experiment the robot starts in the same location with the same orientation.

We compare two different methods for finding a controller for a given body plan: random sampling and learning.

#### Random Sampling

For this experiment, Elman networks with 8 hidden neurons are randomly initialized with *LHS* for each body plan. This experiment is used as a benchmark and to identify whether any body plans can solve tasks with random controllers. A total of 100 random controllers are generated for each robot in the bootstrap population. Each evaluation has a length of 60 s.

#### Learning

In these experiments, the Novelty-driven Increasing Population Evolutionary Strategy (NIP-ES) algorithm is used to train a controller for each robot in the bootstrap population, based on our previous work [26]. The NIP-ES algorithm is a modified version of the increasing-population Covariance Matrix Adaptation Evolutionary Strategy (IPOP-CMAES) [27]. The IPOP-CMAES algorithm restarts whenever a stopping criterion has been triggered. When the algorithm restarts, the population is doubled. NIP-ES has custom stopping criteria and also includes a novelty score as an additional objective. Complete details of this method, including the stopping criteria and parameter values, can be found in [26].

Learning finishes for a single robot when: (a) the budget of 1000 evaluations has been reached, or (b) the robot has reached the target, or (c) the robot has not moved in 50 evaluations. The robot has reached the target when the robot is 0.141 m away from the target which is equal to a fitness of 0.95 (the fitness is normalised using the maximum distance possible in the arena, namely the diagonal of the arena: 2.82 m). The length of each evaluation is 60 s.

As in the previous experiment, the controller is an Elman network with 8 hidden neurons and context units. The number of inputs corresponds to two times the number of sensor organs on the body plan, because each sensor organ outputs two signals (see Section 3.1.1). The number of outputs is equal to the number of actuators, i.e., number of joints and wheels.

### 3.3.1. Experiments and Results

The objective of the experiments in this section is to evaluate and identify the necessary attributes in the robots to solve the environments. For this, the *clustering-random* method is used to select the bootstrap population for the *feature* descriptor and the *LHS* descriptor. The latter descriptor is used as a benchmark. A total of 15 repetitions are shown in this section.

#### Random Sampling of Controllers

In this experiment, 100 random controllers are generated with LHS for each robot in the bootstrap population. These robots are then evaluated in each environment (Figure 6). The length of each evaluation is 60 s. The results can be found in Table 6 and are described next.

The *feature* descriptor provides the highest number of robots closer to the target for any environment, and this is because of the diversity in the population. The *empty arena* has the highest number of robots reaching the target. This is because it is the easiest task, with no obstacles in the way, therefore the likelihood of reaching the target is high. This is not true for the *escape room* and *middle wall*, where robots require more complex controllers and body plans to solve these environments.

**Table 6.** Bootstrap population evaluation with 100 controllers selected at random from robot populations evolved using (a) random sampling, (b) evolution with feature descriptor (as described in Section 3.1.2). The values show the median number of robots that reach a distance  $x$  from the target. It is clear that selecting from the population evolved using the *feature* descriptor leads to more robots that are able reach the target distance in each case. The standard deviation is shown in parentheses. Shaded cells represent the best values.

Distance from Target	Body Plan Random Sampling			Evolution with <i>feature</i> Descriptor		
	Empty Arena	Escape Room	Middle Wall	Empty Arena	Escape Room	Middle Wall
0.141 m	0 (0.4)	0 (0.3)	0 (0.3)	1 (2.1)	0 (1.2)	0 (0.5)
0.25 m	0 (0.4)	0 (0.3)	0 (0.3)	1 (2.1)	0 (1.2)	0 (0.5)
0.5 m	1 (1.4)	2 (1.2)	0 (0.4)	4 (3.5)	2 (3.2)	1 (1)
0.75 m	15 (3.7)	16 (2.7)	3.5 (1)	27 (4.8)	22 (5)	11 (4.8)

The number of robots with different organ combinations are illustrated in Figure 7. Most robots in all the bootstrap populations have only one wheel or one joint (top figure). The main attribute required for the robots to get close to the target in the *empty arena* is to have wheels. This is because the robots can orbit their way to the target. For the *escape room*, some robots need joints to reach the target. Wheeled robots get trapped by walls easily, whereas robots with joints are less affected by this. Robots need two wheels to solve the middle wall environment, as differential drive robots are easier to control to solve this kind of problem.

The robots that have a good performance in a simple environment (empty arena) seem to also have a relatively high performance in more complicated environments (escape room and middle wall). Figure 8 shows the performance of each robot in one bootstrap population. Some robots that did well in the empty arena keep doing well in the escape room and in the middle wall room, just with a reduction in performance. This reduction in performance might be caused by (1) the controller not being good enough to solve the second environment and/or, (2) the physical attributes of the robots not being suitable for the second environment.

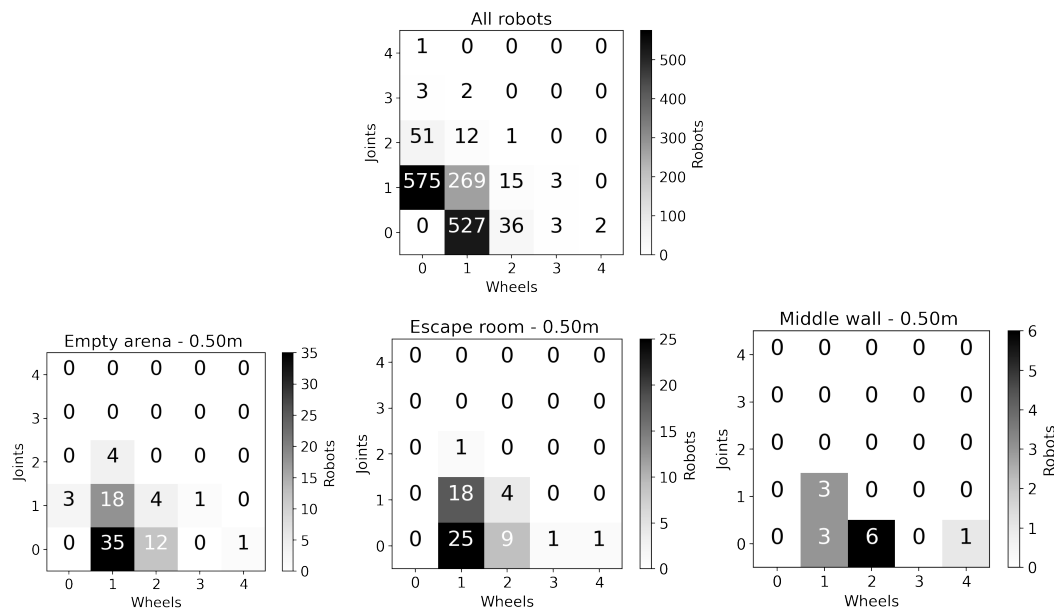


**Figure 7.** The number of robots with different combinations of organs. The top plot shows all the robots in all the bootstrap populations. The bottom figures show only the robots that got within 0.5 m of the target for the empty arena, escape room and the middle wall mazes, respectively.

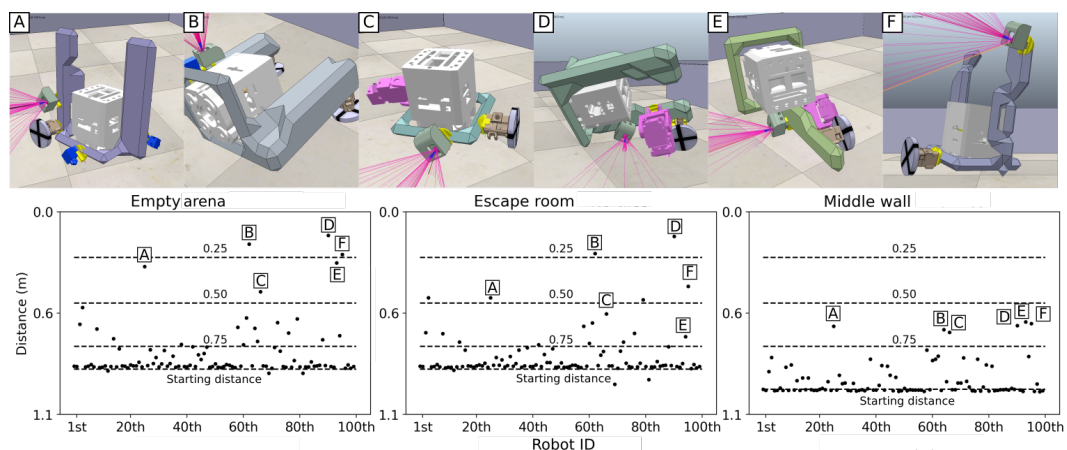


**Figure 8.** Evaluation of each robot of a single bootstrap population for the empty arena, the escape room and the middle wall. The performance of the same 6 robots (A–F) changes from one environment to another.

In conclusion, the body plans play a key role in solving the navigation task in different environments. Wheeled robots are shown to have a good performance in solving the given environments.

### Learning a Controller for a Body Plan

A learning algorithm (NIP-ES) with a budget of 1000 evaluations was applied to each robot in the bootstrap population to gain more insight into the quality of each body plan and identify the ratio of robots able to solve the navigation task. The experiments were conducted first with a bootstrap population obtained through random sampling, and then with a population obtained using novelty search. Robots were selected using the *cluster-random* method in each case.

As shown in Table 7, in the histograms of Figure 9, and in Figure 10, there are more robots able to complete the task in the populations obtained with novelty search compared to those formed by random sampling. Table 7 shows the median number of robots able to approach the beacon at a distance less than 0.75, 0.5, 0.25 and 0.141 m. 0.141 m corresponds to a fitness of 0.95, which is the



minimum value required to complete the task. With either a budget of 100 or of 1000 evaluations, there are in both cases significantly more robots in each distance category than in the case of the randomly sampled robots.

**Table 7.** Bootstrap population evaluation with learning using NIP-ES with a budget of 1000 evaluations from robot populations evolved using (a) random sampling (b) evolution with feature descriptor (as described in Section 3.1.2). The values show the median number of robots that reach a distance  $x$  from the target. The values in parentheses are the standard deviations. The distance of 0.141 m corresponds to the fitness 0.95 which is the minimal value required to complete the task. The values highlighted are the greater value between the random sampling and the evolution with feature descriptor.

	Distance from Target	Body Plan Random Sampling			Evolution with feature Descriptor		
		Empty Arena	Escape Room	Middle Wall	Empty Arena	Escape Room	Middle Wall
1000 evaluations	0.141 m	4 (1.4)	3.5 (1.4)	1 (0.9)	7 (2.3)	4 (2.4)	2 (1)
	0.25 m	6 (2)	5 (1.4)	2 (1.1)	9 (2.7)	6 (2.6)	2 (0.8)
	0.5 m	11 (2.4)	10 (2.6)	3 (1.4)	15 (3.7)	12 (3.2)	5 (2.1)
	0.75 m	17 (3.2)	17 (3.5)	19 (3.3)	25 (4.2)	24 (4.0)	28 (5.5)
100 evaluations	0.141 m	1 (0.8)	1 (0.7)	0 (0.3)	1 (1.5)	1 (0.9)	1 (0.9)
	0.25 m	2 (1.2)	1 (0.9)	0 (0.3)	3 (1.5)	1 (1.2)	1 (0.9)
	0.5 m	4 (1.7)	2 (1)	0 (0.7)	5 (2.7)	4 (2)	1 (1.7)
	0.75 m	10 (1.9)	9 (2.4)	11 (3)	13 (3.5)	12 (2.9)	15 (4.5)

Moreover, the diversity of body plans in terms of number of wheels and joints is greater in the population obtained with evolution as shown in Figure 9, which shows the number of robots sorted by their numbers of wheels and joints. The first two rows correspond to the population obtained with evolution, and the last two rows the body plans obtained by random sampling. The histograms also show the number of robots capable of completing the task with budgets of 100 and 1000 evaluations.

Finally, these results are confirmed by Figure 10 which shows the best fitness for all the body plans of all replications. There are more robots able to move in the population obtained with evolution than with random sampling: 841, 847 and 903 with evolution versus 708, 705 and 729 with random sampling in the empty arena, escape room and middle wall, respectively.

A side result of the experiments described in this section is to observe the benefit of using learning over just sampling controllers randomly. The NIP-ES algorithm with only 100 evaluations is able to find more robots that complete the task than with the 100 random-sampled controllers shown in the previous section (see Figures 7 and 9 and Tables 6 and 7). However, 1000 evaluations is needed to reach the full potential of learning. The number of robots that complete the task with 1000 evaluations is nearly 4 times higher than with 100 evaluations. Moreover, the number of robots and the diversity of their body plans are higher with the population obtained by evolution than the one obtained by random sampling.

Figure 11 shows fifteen examples of robots' body plans. The first row corresponds to the successful robots, the second row corresponds to the robots that can move but cannot reach the target and the last row corresponds to the robots that are incapable of moving. Thus, this figure highlights the diverse set of body plans produced by the body plan generation step. As shown in Figure 9, the number of wheels plays an important role in solving a navigation task. The first row shows the robots with multiple wheels on the ground, and each of these robots have a fitness above 0.95 in all the three environments. The second row shows only robots with one wheel, and the fitness of each robot is more variable in all the three environments. Lastly, the third row shows robots with no actuators that touch the ground.

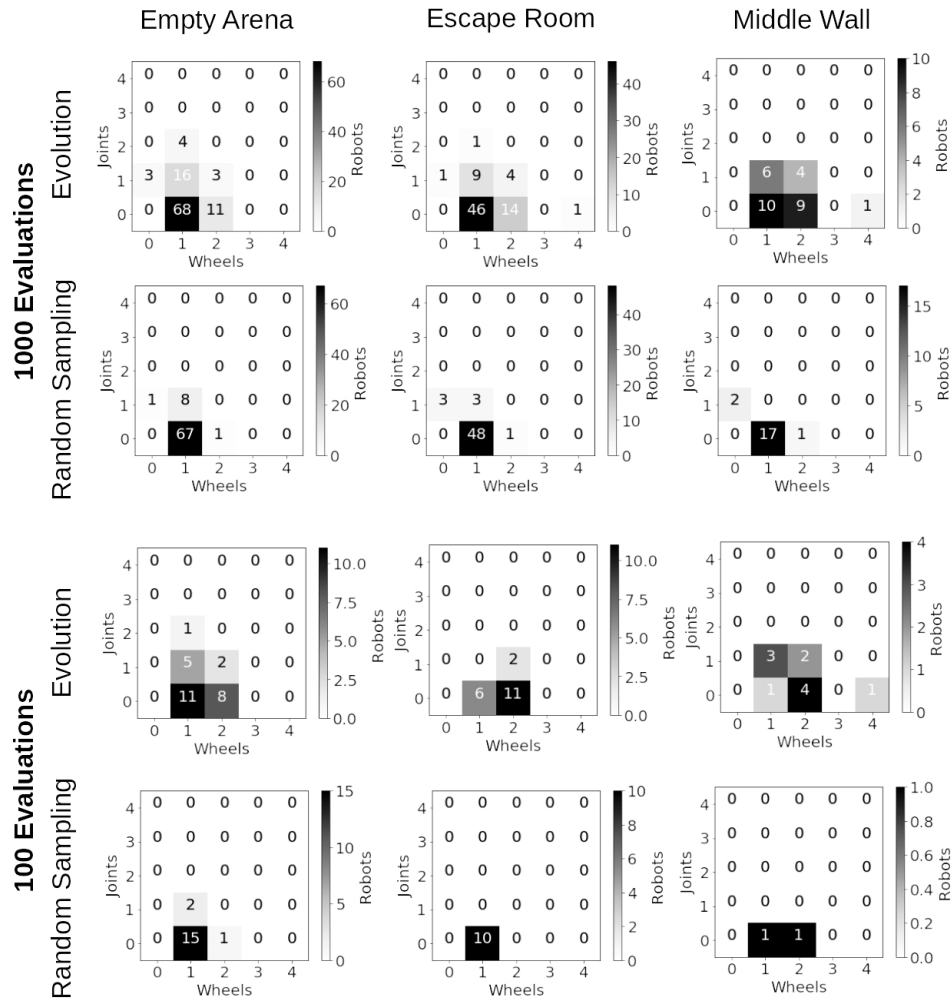


**Figure 9.** Histograms of the number of robots with different combinations of wheels and joints. In the first and third row, the body plans come from the populations obtained with the evolution using the *feature* descriptor, and in the second and fourth row they are obtained by random sampling. Both are selected using the *cluster random* method. The histograms are shown for a budget of 1000 and 100 evaluations of Novelty-driven Increasing Population Evolutionary Strategy (NIP-ES).

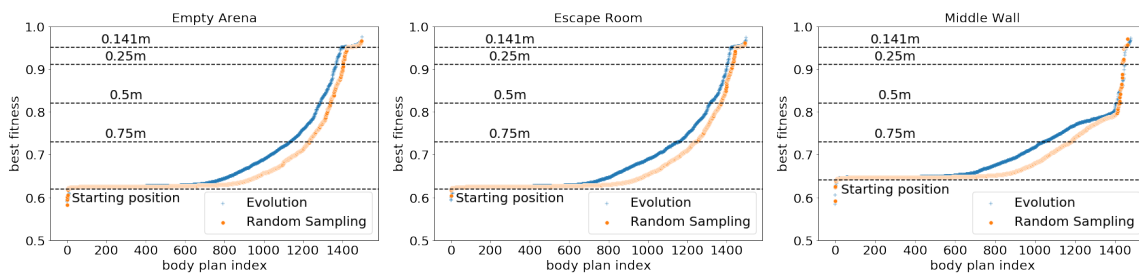


**Figure 10.** The best fitnesses for each body plan of the bootstrap population for all the replicates. The body plans are sorted from the lowest best fitness to the highest for readability. Robots evolved with the *feature* descriptor are shown in blue, and the population produced with random sampling shown in orange. Both populations were selected using the *cluster-random* method.

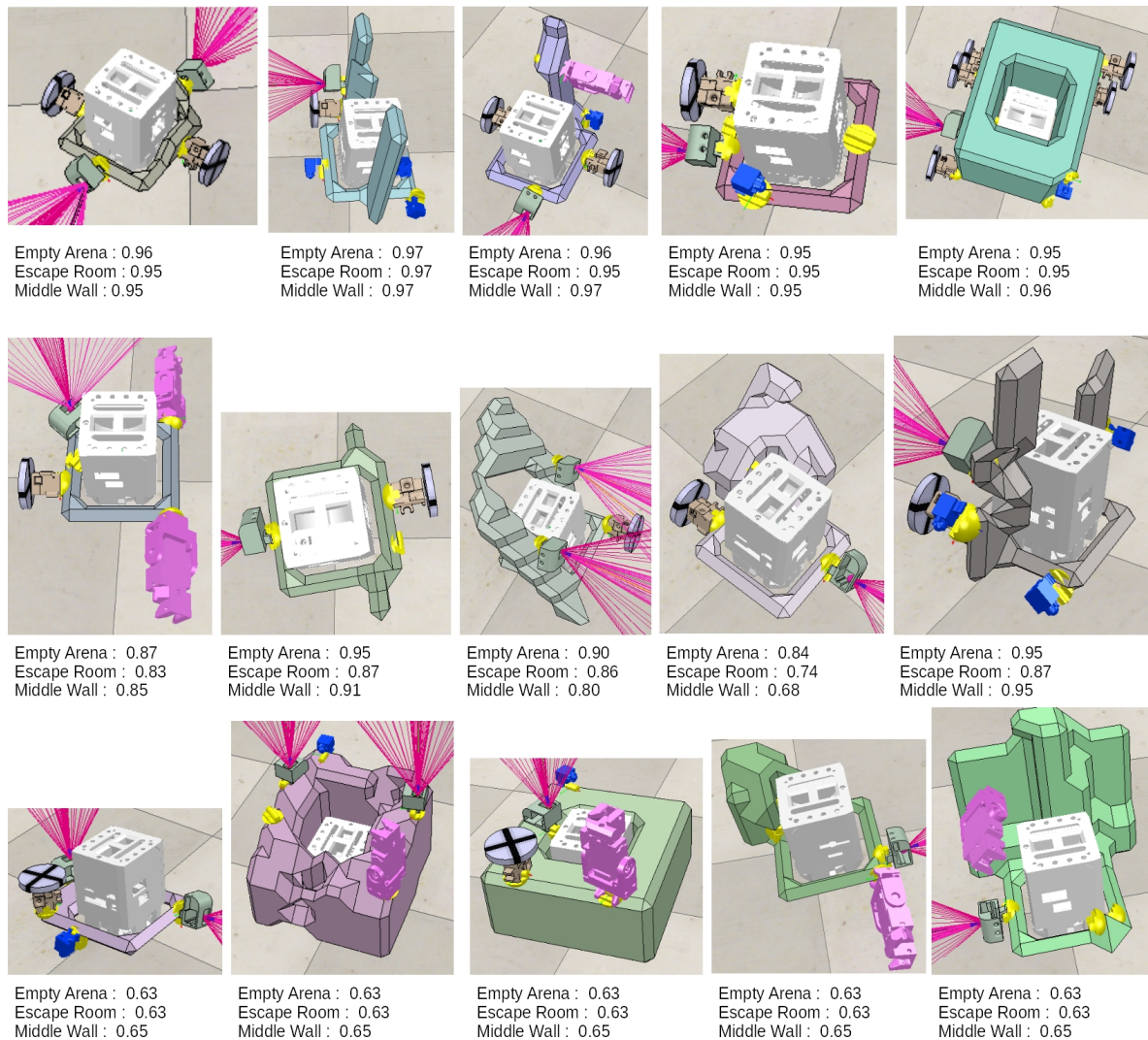


**Figure 11.** This figure shows 15 robots with their performance in each environment. The robots in the upper row had a good performance, the robots in the middle row had medium performance and the robots in the bottom row had a low performance. Under each picture is written the fitness of the robot in each environment.

### 3.4. Body Plan + Controller Evolution

In order to investigate whether a morph-neuro evolutionary algorithm that simultaneously evolves both body plan and control can be improved by bootstrapping in the manner described above, we conduct further experiments using the following method.

The genome of each robot in the population is divided into two parts: a body plan and a controller. The body plan part follows the same architecture as shown in Section 3.1.1. The Hyper-NEAT algorithm is used to evolve the controller [28]. Each body plan is linked with a controller that is indirectly encoded using a CPPN. The decoded controller is a feed-forward neural network with 4 hidden neurons. The decoding takes place as follows.

A feed-forward neural network is produced by connecting the inputs from the sensors with the output of the joints and wheels. The CPPN generates the weights of these connections. For this, the coordinates of the sensors and the actuators are used as input for the CPPN, and the output defines the weight between these connections. A CPPN can thus be used to generate the neural network for any type of body plan, regardless of the number of inputs and/or outputs.

### 3.4.1. Experiment and Results

In this section, the body plan and the controller for each robot are evolved. The body plan and the controller are each encoded in a separate CPPN. During evolution, operators are applied separately to each CPPN. Figure 12 shows fitness, coverage and distribution convergence plots for all the environments (empty arena, escape room and middle wall).

The fitness convergence plots are shown in the left column from Figure 12, where fitness measures the proximity of a robot to the target. In the empty arena and middle wall environments, the bootstrap method results in a higher fitness and diversity than that of a randomised starting population. However, in the escape room, it appears that there is no difference between these two methods (bootstrap population and randomised population). This might be because it is difficult for the robots to reach the target, given that the robots are relatively big: this means they can become trapped by, or stuck on the walls, making it harder for the evolution to converge to a high-fitness solution. Therefore, in this instance, the bootstrap population method does not show any advantage. This is consistent with the results shown in Tables 6 and 7 and Figure 11, where the robots in the escape room exhibit a lower performance than the robots in the empty arena and middle wall environments.

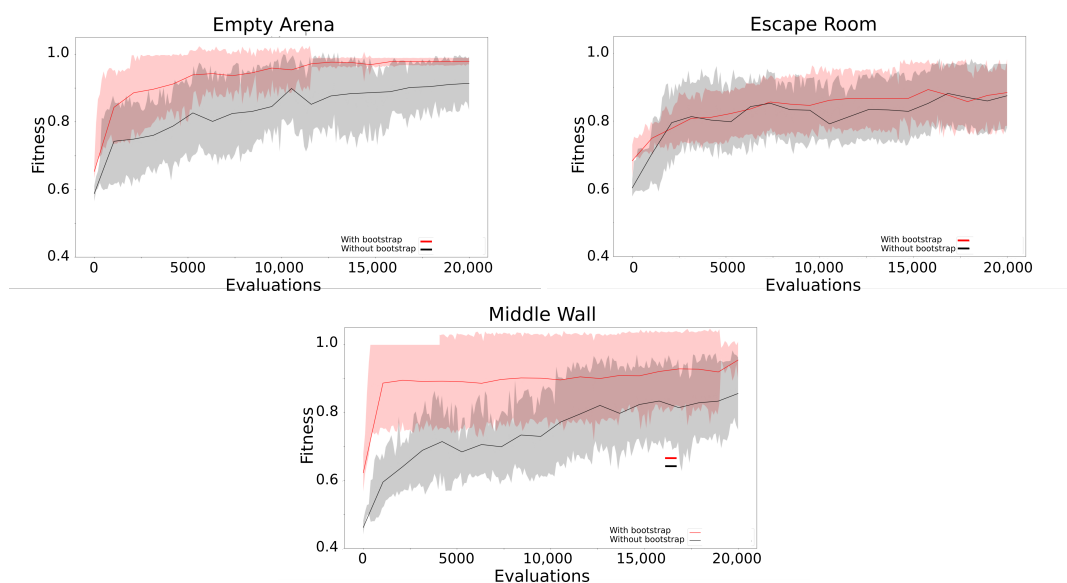


**Figure 12.** The fitness curve of the body plan + controller evolution experiments for the empty arena, escape room and middle wall. Experiments with the bootstrap population take fewer evaluations to converge to a solution than with a random initial population for the empty arena and the middle wall.

Overall, the use of the bootstrap population appears to decrease the number of evaluations required for the evolution to converge to a solution. In addition, the coverage of the body plan search space is higher with the bootstrap than with a randomized population.

### 3.5. From Virtual to Physical: Fabricating Robots

The main goal of this section is to present some examples of fabricated physical robots (The performance of the physical robots has not been evaluated, as the organs are still in development.) from virtual evolved robots. The robots are shown in Figure 13, demonstrating that virtual evolved robots with different features can be fabricated in the physical world.

The robot in the first column had the best performance of the three robots shown. This is because this robot evolved a two-wheeled differential-drive mechanism, and this kind of robot has been proven to be relatively easily to control. The robot in the second column had a better performance than the previous one. The robot falls over because all the mass is concentrated in the top part. The robot uses the wheel to move in the environment and the joint organ to change direction. The robots in the third



column had poor performance in the simulations. This is because the only behaviour this robot can have is to rotate on the spot.

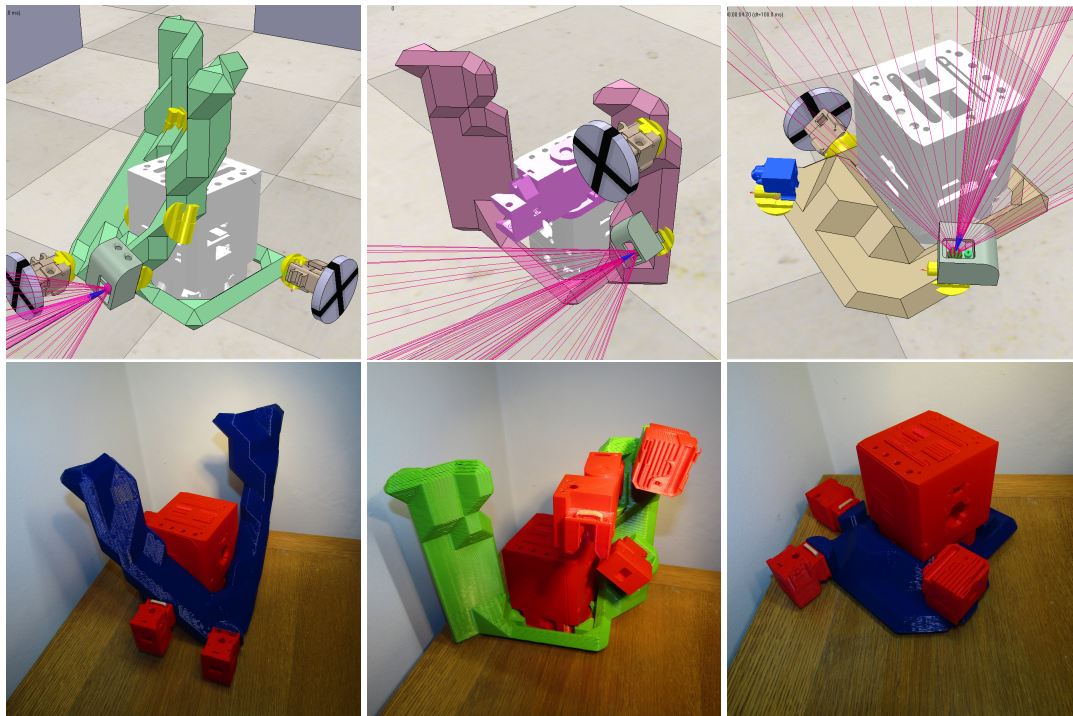


**Figure 13.** Examples of robots evolved, where the virtual models are shown in the top row and physical robots in the bottom row. The physical robots in the bottom row only represent the skeleton and the performance of the physical robots was not evaluated. The robot in the first column has a good performance as this robot was evolved as a differential wheeled robot. The robot in the second column has a better performance as it can use the joint to change direction. The robot in the third column has a bad performance as it can only rotate on the spot.

#### 4. Discussion

In this paper, a novel method to generate a bootstrap population of diverse robots that can be autonomously fabricated is introduced. There are three evolutionary processes at play. First, a novelty search algorithm is used to evolve a large list of robots, from which a subset of robots is selected to form a bootstrap population. Secondly, a learning algorithm (NIP-ES, [26]) is applied to the bootstrap population to learn a controller for these robots, to gain insight into the potential capabilities of the bootstrap population. Finally, the bootstrap population (of body plans) is used to form the initial population of an evolutionary algorithm by pairing each body plan with a random CPPN that generates a controller. Starting from this bootstrap population, an evolutionary algorithm is run to find a robot capable of solving a maze navigation task, simultaneously evolving both body plans and controllers. The key results from this paper are described next.

*The choice of body plan descriptor influences the complexity and diversity of the body plans evolved (Section 3.1.3).* Used in conjunction with novelty search, the descriptor defines the physical attributes of a robot, including skeleton complexity and the number and type of organs. In this paper, the robots were evolved for novelty with three different descriptors: *feature*, *symmetry* and *spatial*. The most complex skeletons were evolved with the *spatial* descriptor as more of the elements of the descriptor are associated with the skeleton properties. The *feature* descriptor provided the highest number of robots with different numbers of organs and this is because the organs have a heavier weight in this descriptor. The *symmetry* descriptor sits somewhere between these. The body plan descriptor plays a key role defining the final physical properties in the robots. Therefore, the body plan needs to be carefully designed to suit the task for the robots.



*The method used to select the bootstrap population influences the final diversity and numbers of organs in the population (Section 3.2.1)*—Four different algorithms to select the bootstrap population were compared (LHS, clustering-random, clustering-sorting and sparseness-sorting) with the k-means clustering algorithms providing the best bootstrap populations with the highest number of diverse robots. LHS was the method with worst performance. The clustering algorithms were able to successfully classify the robots in clusters with different properties according to the traits in the *feature* descriptor.

*Body plans evolved with the feature descriptor exhibit better navigation behaviours with both randomly assigned controllers and learned controllers than body plans that are randomly generated (Section 3.3.1).* The behaviours of the robots in the final bootstrap populations were evaluated in three different environments, with randomly generated controllers and with a learner, and this was compared with randomly generated robots. The evolved body plans had a higher number of robots getting closer to the target than the randomly generated body plans. This means that the bootstrap population are diverse enough to have enough body plans to solve the environments for this paper without the need to evolve the body plan any further. For more complex environments, further evolution of the body plan might be required.

*Bootstrapping an EA with an initial population selected for diversity reduces the number of evaluations necessary to converge to the solution, when a population of robots with controllers and body plans is evolved (Section 3.4.1).* It takes a larger number of evaluations for an evolutionary loop to converge to a good solution with a random initial population than with a population evolved for novelty. This is because when robots are evolved for novelty, there is high likelihood that one of the robots in the population will have a good performance in the environment, as the population is more diverse. The reduction in number of evaluations will become very important when robots are evolved for more complex environments.

Overall, the body plan generation creates a better initialisation population than a population generated at random. The evolved populations are diverse enough to have some body plans in the population that are capable of solving some environments without the need of further optimisation. In addition, an evolutionary loop starting with a bootstrap population converges quicker to the solution than with an initial population generated at random. Finally, all of the robots in the experiments can be autonomously fabricated by the Robot Fabricator.

## 5. Concluding Remarks

Employing artificial evolution for discovering well-performing and novel robots for complex environments and tasks has great potential [29–32]. However, forced by technical limitations, existing work in evolutionary robotics is mainly limited to simulations and the physically constructed robots—if any—are very simple. Thus, the transition from the virtual domain to the real world is yet to be made.

The Autonomous Robot Evolution project represents a milestone on the long road ahead. The overall goal of the project is to make the transition to the real world and develop a system where physical robots evolve. A key objective to this end is to automate the fabrication of complex robots with partly 3D-printed bodies, a CPU and several sensors and actuators. The hands-free fabrication of robots is difficult, but the technology is becoming available [2,8,9].

In this paper, we identify a new problem that does not occur in simulated evolutionary processes. This problem, dubbed the fabrication challenge, is rooted in the fact that autonomous robot reproduction inevitably implies constraints regarding the evolved robots. In short, the robots need to be not only be conceivable but also autonomously fabricated. This implies an essential condition for the robotic evolution process: the initial population needs to consist of manufacturable and diverse robots. The chief contribution of this paper is a novel method to generate this initial population. To be specific, we describe and investigate a method that considers not only morphological constraints but also behavioural requirements of the generated body plans and the diversity within the set of generated body plans. To assess the merits of this method, we ran a full robot evolutionary process

where the morphologies (body plans) and the controllers (brains) of the robots were evolved together. The experiments showed that initialising the first generation by our method improves the efficiency and the efficacy of evolution.

In this method, a large pool of diverse manufacturable robots is generated. Then, a subset of diverse and viable robots is selected from this list to seed the evolutionary process. The results shown in this paper can be summarised as follows: (a) the descriptor used defines the physical attributes of the final list of robots evolved; (b) the method used to select the subset of robots (population) define the diversity of the same population; (c) the initialization of the population is better with a pre-evolved list of robots than a random population and (d) the speed of convergence increases when the initial population is selected from evolved robots.

Further work will explore the enhancement of the genome decoder, with the goal of increasing the number of organs generated in the evolved robots. In addition, new methods of evolution of body plans and controllers will be explored. Most importantly, the physical robots will be evaluated in a real-world setup and any resulting reality gap measured, with the objective of then developing new methods to decrease it.

**Author Contributions:** The individual contribution for this article were as follows: Conceptualization: E.B., L.K.L.G., E.H., A.E.E., W.L., J.T., A.M.T.; methodology: E.B., L.K.L.G., E.H., A.E.E., W.L., J.T., M.F.H., M.A., R.W., A.M.T.; software: L.K.L.G., E.B., W.L., M.D.C.; validation: E.B., L.K.L.G., W.L.; formal analysis: E.B., L.K.L.G., W.L.; investigation: E.B., L.K.L.G., W.L.; visualization: E.B., L.K.L.G., E.H., A.E.E., W.L., J.T., A.M.T.; supervision: E.B., E.H., A.E.E., J.T., A.M.T.; project administration: E.H., A.E.E., J.T., A.M.T.; funding acquisition: E.H., A.E.E., J.T., A.F.W., A.M.T.; writing—original draft: E.B., L.K.L.G., E.H., A.E.E., W.L., A.F.W., R.W., M.F.H., A.M.T. All authors have read and agreed to the published version of the manuscript.

**Funding:** This work is funded by EPSRC ARE project, EP/R03561X, EP/R035733, EP/R035679, and the Vrije Universiteit Amsterdam.

**Conflicts of Interest:** The authors declare no conflict of interest.

## Abbreviations

The following abbreviations are used in this manuscript:

ARE	Autonomous Robot Evolution
EA	Evolutionary Algorithm
NS	Novelty Search
LHS	Latin Hypercube Sampling
CPPN	Compositional Pattern Producing Networks
NIP-ES	Novelty driven Increasing Population Evolutionary Strategy
IPOP-CMAES	Increasing Population Covariance Matrix Adaptation Evolutionary Strategy

## Appendix A. Sparseness Metric

The sparseness metric in Equation (A1) [22] measures the novelty of a single body plan.  $k$  represents the number of closest neighbours in the archive,  $\mu_i$  represents neighbour  $i$  and the  $dist$  function represents the Euclidean distance between two descriptors. A value of 15 for  $k$  has been previously shown to provide good results [33] and is used in all experiments.

$$\rho(x) = \frac{1}{k} \sum_{i=0}^k dist(x, \mu_i), \quad (A1)$$

An archive is used to collect the descriptors if they meet one of the following conditions. Firstly, each descriptor  $x$  has a probability  $P(x) = 0.1$  of being added to the archive automatically. Second, a descriptor is added if the sparseness value  $p(x)$  is greater than 0.2 ( $p(x) > 0.2$ ).

## Appendix B. Coverage Metric

To measure the diversity of the population, we use two complementary metrics: *coverage* and *uniformity*. Similar metrics are used in previous studies [33–35] to assess the quality of a novelty search output. The *coverage* measures how much the search space is covered by the population. To this end, the descriptor space is discretised into a grid of a fixed number of bins (5 bins per dimension is used here). Then, the number of cells with at least one individual is counted and divided by the total number of cells to be normalized (see Equation (A2)).

$$n_r(P) = |\{c_i > 0\}|$$

$$C(P) = \frac{n_r(P)}{n} \quad (A2)$$

where  $P$  is the population;  $n_r$  the number of cells with at list one individual;  $c_i$  the count of individual in cell  $i$ ;  $n$  the total number of cells.

Within the covered space, the *uniformity* measures the distance between an ideal uniformity distribution and the population's descriptors distribution. The Jensen–Shannon divergence is used as a distance [36]. The covered space corresponds to the hyper-cube enveloping the cells containing the population.

$$D_u = \left\{ \frac{1}{n_r(P)} \right\}_I$$

$$D(P) = \left\{ \frac{c_i}{|P|} \right\}_I \quad (A3)$$

$$U(P) = 1 - JSD(D_u, D(P))$$

where  $I$  is the index of the cells in the covered space,  $D_u$  the uniform distribution,  $D(P)$  the population's descriptors distribution and  $JSD$  the Jensen–Shannon divergence.

## Appendix C. Robot Coverage for the Body Plan + Controller Evolution

Figure A1 shows the coverage curve (Appendix B). Notice that the curves are smoothed using b-spline method over original data points to better illustrate the overall trending. Overall, experiments with the bootstrap population start with a higher diversity but it drops after a couple hundreds of evaluations. This is because of the nature of the evolutionary algorithm which promotes convergence rather than diversity. However, this is not the case with uniformity.

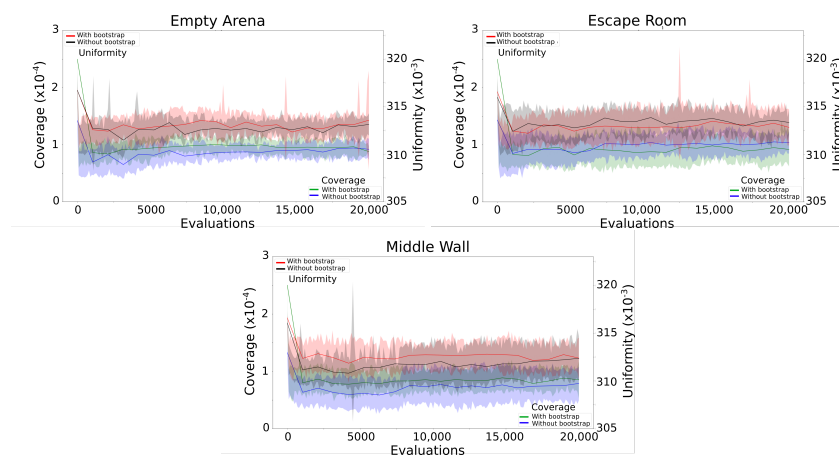


**Figure A1.** The diversity curve of the body plan + controller evolution experiments for the empty arena, escape room and middle wall. The coverage is higher at the beginning for the experiments with the bootstrap population and it decreases.

## References

1. Eiben, A.; Hart, E.; Timmis, J.; Tyrrell, A.; Winfield, A. Towards Autonomous Robot Evolution. In *Software Engineering for Robotics*; Cavalcanti, A.L.C., Dongol, B., Hierons, R.H., Timmis, J., Woodcock, J.C.P., Eds.; Springer: Berlin/Heidelberg, Germany, 2021.
2. Hale, M.F.; Buchanan, E.; Winfield, A.F.; Timmis, J.; Hart, E.; Eiben, A.E.; Angus, M.; Veenstra, F.; Li, W.; Woolley, R.; et al. The ARE Robot Fabricator: How to (Re) produce Robots that Can Evolve in the Real World. In *Proceedings of the 2018 Conference on Artificial Life: A Hybrid of the European Conference on Artificial Life (ECAL) and the International Conference on the Synthesis and Simulation of Living Systems (ALIFE)*, Newcastle, UK; MIT Press: Cambridge, MA, USA, 2019; pp. 95–102.
3. Lipson, H.; Pollack, J.B. Automatic design and manufacture of robotic lifeforms. *Nature* **2000**, *406*, 974–978. [[CrossRef](#)] [[PubMed](#)]
4. Brodbeck, L.; Hauser, S.; Iida, F. Morphological evolution of physical robots through model-free phenotype development. *PLoS ONE* **2015**, *10*, e0128444. [[CrossRef](#)] [[PubMed](#)]
5. Jelisivcic, M.; De Carlo, M.; Hupkes, E.; Eustratiadis, P.; Orlowski, J.; Haasdijk, E.; Auerbach, J.E.; Eiben, A.E. Real-world evolution of robot morphologies: A proof of concept. *Artif. Life* **2017**, *23*, 206–235. [[CrossRef](#)] [[PubMed](#)]
6. Kriegman, S.; Blackiston, D.; Levin, M.; Bongard, J. A scalable pipeline for designing reconfigurable organisms. *Proc. Natl. Acad. Sci. USA* **2020**, *117*, 1853–1859. [[CrossRef](#)] [[PubMed](#)]
7. Long, J. *Darwin's Devices: What Evolving Robots Can Teach Us about the History of Life and the Future of Technology*; Basic Books: New York, NY, USA, 2012.
8. Hale, M.F.; Angus, M.; Buchanan, E.; Li, W.; Woolley, R.; Le Goff, L.K.; de Carlo, M.; Timmis, J.; Winfield, A.F.; Hart, E.; et al. Hardware Design for Autonomous Robot Evolution. In *IEEE Symposium Series on Computational Intelligence*; IEEE: Canberra, Australia, 2020; in press.
9. Buchanan, E.; Le Goff, L.; Hart, E.; Eiben, A.E.; de Carlo, M.; Li, W.; Hale, M.F.; Angus, M.; Woolley, R.; Winfield, A.F.; et al. Evolution of Diverse, Manufacturable Robot Body Plans. In *IEEE Symposium Series on Computational Intelligence*; IEEE: Canberra, Australia, 2020; in press.
10. Eiben, A.; Kernbach, S.; Haasdijk, E. Embodied Artificial Evolution—Artificial Evolutionary Systems in the 21st Century. *Evol. Intell.* **2012**, *5*, 261–272. [[CrossRef](#)] [[PubMed](#)]
11. Eiben, A.; Bredeche, N.; Hoogendoorn, M.; Stradner, J.; Timmis, J.; Tyrrell, A.; Winfield, A. The triangle of life: Evolving robots in real-time and real-space. In *Proceedings of the 12th European Conference on the Synthesis and Simulation of Living Systems (ECAL 2013)*, Taormina, Italy, 2–6 September 2013; Lio, P., Miglino, O., Nicosia, G., Nolfi, S., Pavone, M., Eds.; MIT Press: Cambridge, MA, USA, 2013; pp. 1056–1063.
12. Koos, S.; Mouret, J.B.; Doncieux, S. The transferability approach: Crossing the reality gap in evolutionary robotics. *IEEE Trans. Evol. Comput.* **2012**, *17*, 122–145. [[CrossRef](#)]
13. Bongard, J.; Lipson, H. Once more unto the breach: Co-evolving a robot and its simulator. In *Proceedings of the Ninth International Conference on the Simulation and Synthesis of Living Systems (ALIFE9)*, Boston, MA, USA, 12–15 September 2004; pp. 57–62.
14. Pretorius, C.J. *A Comparative Study of Artificial Neural Networks and Physics Models as Simulators in Evolutionary Robotics*; Nelson Mandela University, Faculty of Science: Port Elizabeth, South Africa, 2019.
15. Jakobi, N. Evolutionary robotics and the radical envelope-of-noise hypothesis. *Adapt. Behav.* **1997**, *6*, 325–368. [[CrossRef](#)]
16. Kim, S.; Coninx, A.; Doncieux, S. From exploration to control: Learning object manipulation skills through novelty search and local adaptation. *arXiv* **2019**, arXiv:1901.00811.
17. Kazimipour, B.; Li, X.; Qin, A.K. Initialization methods for large scale global optimization. In *Proceedings of the 2013 IEEE Congress on Evolutionary Computation*, Cancun, Mexico, 20–23 June 2013; pp. 2750–2757.
18. Kazimipour, B.; Li, X.; Qin, A.K. A review of population initialization techniques for evolutionary algorithms. In *Proceedings of the 2014 IEEE Congress on Evolutionary Computation (CEC)*, Beijing, China, 6–11 July 2014; pp. 2585–2592.
19. Stanley, K.O. Compositional pattern producing networks: A novel abstraction of development. *Genet. Program. Evolvable Mach.* **2007**, *8*, 131–162. [[CrossRef](#)]
20. Examples of Evolved Robots. 2020. Available online: <https://youtu.be/xexk9aIsPa4> (accessed on 5 December 2020).

21. Robot Fabricator Assembling Robot. 2020. Available online: <https://youtu.be/mWjZya9PJQg> (accessed on 5 December 2020).
22. Lehman, J.; Stanley, K.O. Abandoning objectives: Evolution through the search for novelty alone. *Evol. Comput.* **2011**, *19*, 189–223. [[CrossRef](#)] [[PubMed](#)]
23. Ye, K.Q. Orthogonal column Latin hypercubes and their application in computer experiments. *J. Am. Stat. Assoc.* **1998**, *93*, 1430–1439. [[CrossRef](#)]
24. MacQueen, J. Some methods for classification and analysis of multivariate observations. In Proceedings of the Fifth Berkeley Symposium on Mathematical Statistics and Probability, Oakland, CA, USA, 21 June–18 July 1965; Volume 1, pp. 281–297.
25. Elman, J.L. Finding structure in time. *Cogn. Sci.* **1990**, *14*, 179–211. [[CrossRef](#)]
26. Le Goff, L.K.; Buchanan, E.; Hart, E.; Eiben, A.E.; Li, W.; de Carlo, M.; Hale, M.F.; Angus, M.; Woolley, R.; Timmis, J.; et al. Sample and time efficient policy learning with CMA-ES and Bayesian Optimisation. In *Artificial Life Conference Proceedings*; MIT Press: Cambridge, MA, USA, 2020; pp. 432–440.
27. Auger, A.; Hansen, N. A restart CMA evolution strategy with increasing population size. In Proceedings of the 2005 IEEE Congress on Evolutionary Computation, Edinburgh, UK, 2–5 September 2005; Volume 2, pp. 1769–1776.
28. Risi, S.; Stanley, K.O. An enhanced hypercube-based encoding for evolving the placement, density, and connectivity of neurons. *Artif. Life* **2012**, *18*, 331–363. [[CrossRef](#)] [[PubMed](#)]
29. Floreano, D.; Husbands, P.; Nolfi, S. Evolutionary Robotics. In *Handbook of Robotics*, 1st ed.; Siciliano, B., Khatib, O., Eds.; Springer: Berlin/Heidelberg, Germany, 2008; pp. 1423–1451.
30. Bongard, J. Evolutionary Robotics. *Commun. ACM* **2013**, *56*, 74–85. [[CrossRef](#)]
31. Vargas, P.A.; Di Paolo, E.A.; Harvey, I.; Husbands, P. *The Horizons of Evolutionary Robotics*; The MIT Press: Cambridge, MA, USA, 2014.
32. Doncieux, S.; Bredeche, N.; Mouret, J.B.; Eiben, A. Evolutionary robotics: What, why, and where to. *Front. Robot. AI* **2015**, *2*, 4. [[CrossRef](#)]
33. Gomes, J.; Mariano, P.; Christensen, A.L. Devising effective novelty search algorithms: A comprehensive empirical study. In Proceedings of the 2015 Annual Conference on Genetic and Evolutionary Computation, Madrid, Spain, 11–15 July 2015; pp. 943–950.
34. Le Goff, L.K.; Hart, E.; Coninx, A.; Doncieux, S. On Pros and Cons of Evolving Topologies with Novelty Search. In *Artificial Life Conference Proceedings*; MIT Press: Cambridge, MA, USA, 2020; pp. 423–431.
35. Doncieux, S.; Paolo, G.; Laflaquière, A.; Coninx, A. Novelty Search makes Evolvability Inevitable. *arXiv* **2020**, arXiv:2005.06224.
36. Endres, D.M.; Schindelin, J.E. A new metric for probability distributions. *IEEE Trans. Inf. Theory* **2003**, *49*, 1858–1860. [[CrossRef](#)]

**Publisher’s Note:** MDPI stays neutral with regard to jurisdictional claims in published maps and institutional affiliations.



© 2020 by the authors. Licensee MDPI, Basel, Switzerland. This article is an open access article distributed under the terms and conditions of the Creative Commons Attribution (CC BY) license (<http://creativecommons.org/licenses/by/4.0/>).